

Ventral hippocampus neurons encode meal-related memory

Received: 18 March 2025

Accepted: 28 April 2025

Published online: 11 June 2025

 Check for updates

Léa Décarie-Spain¹, Cindy Gu¹, Logan Tierno Lauer¹, Keshav S. Subramanian^{1,2}, Samar N. Chehimi³, Alicia E. Kao¹, Serena X. Gao², Iris Deng¹, Alexander G. Bashaw², Molly E. Klug¹, Jessica J. Rea², Alice I. Waldow¹, Ashyah Hewage Galbokke¹, Olivia Moody¹, Kristen N. Donohue¹, Mingxin Yang⁴, Guillaume de Lartigue⁴, Kevin P. Myers⁵, Richard C. Crist³, Benjamin C. Reiner³, Matthew R. Hayes³ & Scott E. Kanoski^{1,2} ✉

The ability to encode and retrieve meal-related information is critical to efficiently guide energy acquisition and consumption, yet the underlying neural processes remain elusive. Here we reveal that ventral hippocampus (HPCv) neuronal activity dynamically elevates between eating bouts during meal consumption and this response is predictive of performance in a foraging-related memory test for the spatial location of a previously consumed meal. Targeted recombination-mediated ablation of HPCv meal-responsive neurons impairs meal location memory without influencing food motivation or spatial memory for escape location. These HPCv meal-responsive neurons project to the lateral hypothalamic area (LHA) and are enriched in serotonin 2a receptors (5HT2aR). Either chemogenetic silencing of HPCv-to-LHA projections or intra-HPCv 5HT2aR antagonist yielded meal location memory deficits, as well as increased caloric intake driven by shorter temporal intervals between meals. Collective results identify a population of HPCv neurons in male rats that dynamically respond during eating to encode meal-related memories.

Encoding and remembering critical information surrounding food consumption is advantageous to efficiently guide future eating behaviors. Foraging, for example, is facilitated by the retrieval of previously stored spatial information about the location of food sources. Even in the modern environment where food is easily accessible, meal-related memories play an important role in the regulation of eating behaviors. For instance, the ability to recall a recent meal robustly influences subsequent hunger and satiety ratings, as well as the amount of food consumed during the next meal^{1–6}.

The hippocampus is a key brain structure for the integration of learning and memory processes with food-seeking and consummatory behaviors⁷. For example, a subnetwork within the human hippocampus implicated in obesity and associated eating disorders

was recently identified⁸. The ventral subregion of the rodent hippocampus (HPCv) is especially responsive to endocrine and neuropeptide signals that regulate metabolism and food intake control^{9–14}, thus making this brain region a prime candidate target for storing meal-related memories. Consistent with this hypothesis, silencing HPCv neurons after food consumption accelerates the onset of a subsequent meal and increases its size^{15,16}, indicating that HPCv neuronal activity in close temporal proximity to a meal influences future eating episodes.

Memory engrams are well characterized for fear-related aversive memories where a specific neuronal ensemble in the amygdala encodes fear memory and its reactivation promotes fear-appropriate behavioral responses^{17–21}. While engrams encoding aversive events are

¹Human & Evolutionary Biology Section, Department of Biological Sciences, University of Southern California, Los Angeles, CA, USA. ²Neuroscience Graduate Program, University of Southern California, Los Angeles, CA, USA. ³Department of Psychiatry, Perelman School of Medicine, University of Pennsylvania, Philadelphia, PA, USA. ⁴Monell Chemical Senses Center, Philadelphia, PA, USA. ⁵Department of Psychology, Bucknell University Lewisburg, Philadelphia, PA, USA. ✉e-mail: kanoski@usc.edu

also formed in the hippocampus^{22–26}, engrams encoding positive reinforcing appetitive events such as cocaine administration²⁷, female exposure^{28,29}, and prosocial interactions³⁰ are formed in this region as well. Despite these advances, the neural circuitry encoding memory engrams pertaining to meal consumption remains to be identified. Here we sought to identify a specific ensemble of meal-responsive HPCv neurons and the mechanisms through which they encode meal-related memory engrams.

Results

Ventral hippocampus neural activity between eating bouts during meal consumption predicts foraging-related memory performance for the spatial location of a previously consumed meal

To determine whether HPCv neurons are dynamically engaged during meal consumption, we expressed the calcium indicator GCaMP7s in the HPCv (Fig. 1a, b) and assessed bulk calcium-dependent activity time-stamped to behavioral events (active eating vs. inter-bout intervals) over the course of a 30 min meal following a 24 h fasting period. Results revealed that CA1v bulk calcium-dependent activity dynamically decreases during active eating bouts and increases during inter-bout intervals (Fig. 1c, d). These results suggest that HPCv activity is engaged during a meal at times when the animals are rearing and observing their environment (periods between active eating bouts). These same rats were then trained in a foraging-related spatial memory test for the location of a previously consumed meal (Fig. 1e) and performance index at the memory probe was positively correlated with the magnitude of calcium-dependent activity increases during the interbout intervals from the prior meal photometry test (Fig. 1f). These findings indicate that HPCv activity dynamics during a meal are functionally connected to memory capacity for meal location.

To identify the subregional anatomical location of HPCv meal-responsive neurons, we employed a “targeted recombination in active population” (TRAP) viral approach to express, following intraperitoneal (ip) administration of 4-hydroxytamoxifen (4OHT; 15 mg/kg; H6278, Sigma-Aldrich, St. Louis, USA), green fluorescent protein (GFP) in HPCv field CA1 (CA1v) neurons expressing cFos following a 24 h fast (“Fasted^{GFP}”), consumption of a 30 min meal (“Fed^{GFP}”), or a 30 min exposure to predator (coyote) urine (“Coyote^{GFP}”) (Fig. 1g, h). Results revealed a significantly greater number of GFP⁺ cell bodies in the Fed^{GFP} versus the Fasted^{GFP} group, no difference in the number of GFP⁺ cell bodies between Fed^{GFP} versus Coyote^{GFP} group, and a trend for a greater number of GFP⁺ cell bodies in the Coyote^{GFP} versus the Fasted^{GFP} group ($p = 0.0797$). The GFP⁺ cells in the Fed^{GFP} state were predominantly located in the pyramidal layer of CA1v (Fig. 1i, j). These results were further confirmed by cFos immunostaining showing significantly enhanced CA1v cFos expression when rats are perfused under a Fed relative to a Fasted state (Extended Data Fig. 1a, b). In addition, the specificity of the TRAP approach to target CA1v meal-responsive neurons was confirmed by greater overlap of cFos and GFP when feeding conditions at the time of 4OHT administration and perfusion are matched versus mismatched in the Fed^{GFP} group (Extended Data Fig. 1c, d). Altogether, these findings indicate that a subset of HPCv neurons (pyramidal CA1v region) display heightened intracellular activity in response to a meal, and that the number of CA1v meal-responsive neurons is comparable to the number CA1v neurons engaged during predator urine exposure but greater than the number engaged during fasting. Further, the activity of these meal-responsive CA1v neurons occurs during the periods between eating bouts when animals have an opportunity to observe the meal environment, and this meal-induced neural response is correlated with foraging-related spatial memory performance for meal location.

Ventral hippocampus meal-responsive neurons encode meal location spatial memory without affecting food motivation, escape location spatial memory, energy balance, or anxiety-like behavior

To investigate the function of CA1v meal-responsive neurons, we modified the previous TRAP viral approach to express diphtheria toxin (dT_A) in CA1v neurons expressing cFos under a Fasted or Fed state (Fig. 2a), leading to dT_A-mediated chronic ablation of CA1v neurons active in response to fasting (Fasted^{dT_A}) or meal consumption (Fed^{dT_A}). These animals were compared to a group undergoing 4OHT-induced expression of GFP in CA1v neurons (Control^{GFP}). No differences in average daily chow intake nor body weight following 4OHT-induced recombination were observed across experimental groups (Extended Data Fig. 2a, b), although chronic loss of CA1v meal-responsive neurons increased meal size relative to the Fasted^{dT_A} and Control^{GFP} groups (Extended Data Fig. 2c) and decreased meal frequency relative to the Control^{GFP} group (Extended Data Fig. 2d) without affecting inter-meal intervals (Extended Data Fig. 2e). We used a foraging-related spatial memory procedure where animals learn to use visuospatial cues to navigate towards the location of a previously consumed meal (Fig. 2b) or an escape-based spatial memory task (Fig. 2c) that employs the same apparatus as the foraging version and is of similar difficulty but is based on memory for escape instead of meal location³¹. In the foraging-related spatial memory task, rats from the Fed^{dT_A} group showed significantly impaired memory performance during a memory probe test for the food location relative to both the Control^{GFP} and Fasted^{dT_A} animals (Fig. 2d–f). Animals from the Fed^{dT_A} group did perform a greater number of investigations relative to the Control^{GFP} group, but no group differences in distance traveled were observed (Extended Data Fig. 2f–h).

To determine whether the impairment in meal-related spatial memory is secondary to the loss of a larger number of neurons in the CA1v in Fed^{dT_A} vs. Fasted^{dT_A} animals, another cohort of animals underwent 4OHT-mediated expression of GFP (Coyote^{GFP}) or dT_A (Coyote^{dT_A}) of CA1v neurons active in response to 30 min exposure to predator (coyote) urine. As indicated above, Fed-TRAP and Coyote-TRAP approaches targeted a comparable number of CA1v neurons (Fig. 1i, j). Results revealed that rats from the Coyote^{dT_A} group did not differ from Coyote^{GFP} animals during either the acquisition phase (Fig. 2h, i) or the memory probe test (Fig. 2j). No group differences were observed in distance traveled nor the number of investigations (Extended Data Fig. 2i–k). These findings indicate that loss of CA1v neurons responsive to a fear-associated non-appetitive event—and with a similar number of neurons ablated compared to Fed^{dT_A} animals—does not affect foraging-related spatial memory.

To assess the selectivity of CA1v ablated neurons in Fed^{dT_A} animals in mediating spatial memory for meal location (vs. spatial memory in general), another cohort of animals underwent the same meal-related ablation or control treatment as with the previous cohort, before training in the escape-based spatial memory task. In this case, Fed^{dT_A} rats did not differ from Control^{GFP} animals during escape location training (Fig. 2l, m) nor during the memory probe test (Fig. 2n). The overall distance traveled, and number of investigations were similar across groups (Extended Data Fig. 2l–n). Thus, meal-responsive CA1v neurons appear to selectively mediate memory associated with meal consumption.

It is possible that the memory impairment in the food-reinforced spatial task in rats with meal-responsive CA1v neurons ablated was secondary to elevated anxiety-like behavior and/or motivation for the sucrose reinforcer, as this brain region is associated with both anxiety^{32,33} and food motivation^{34,35}. To test this, a similar cohort of animals was tested in an effort-based operant lever pressing for sucrose rewards (progressive ratio reinforcement schedule), as well as the zero maze test for anxiety-like behavior. Results reveal no group

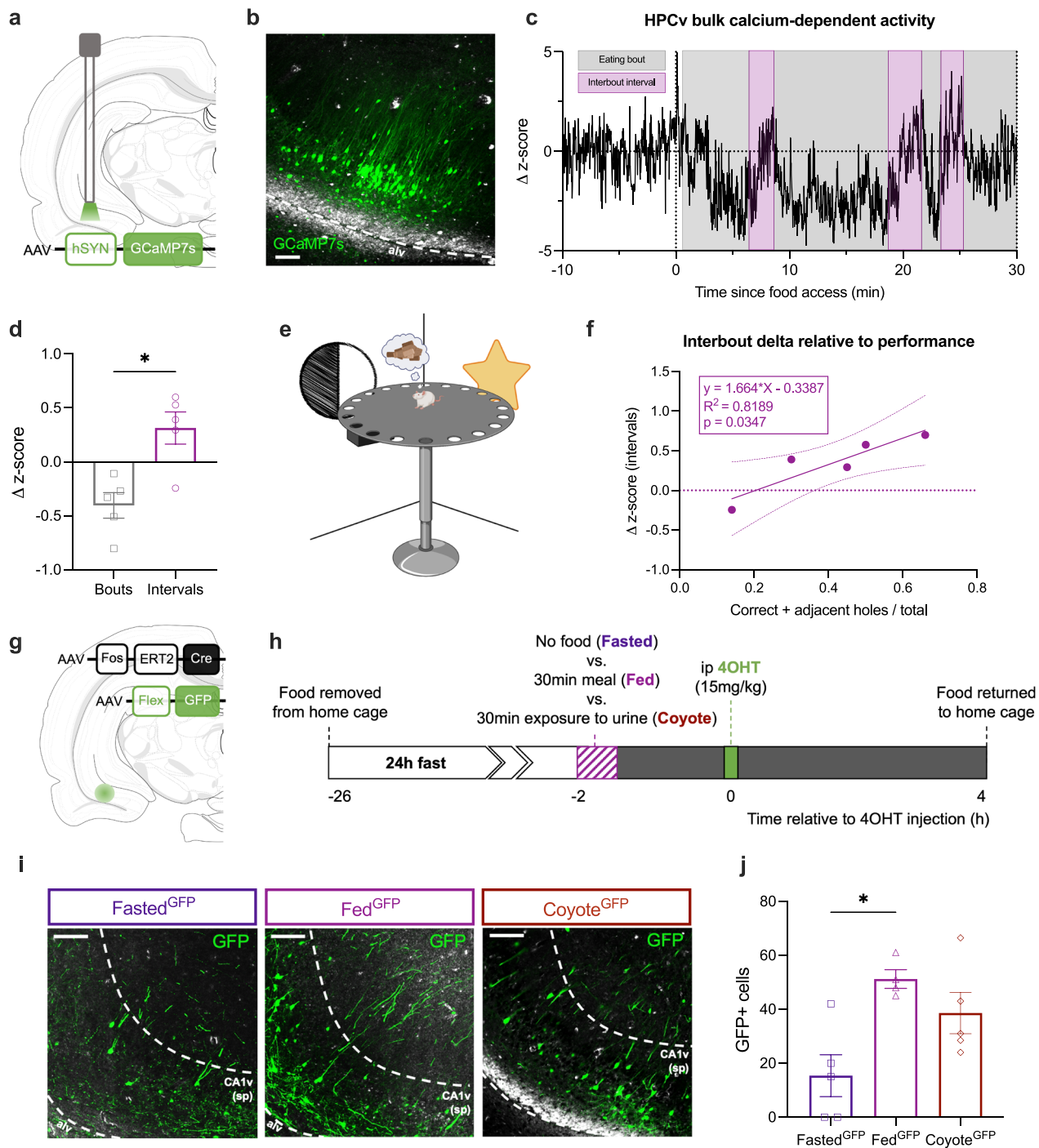
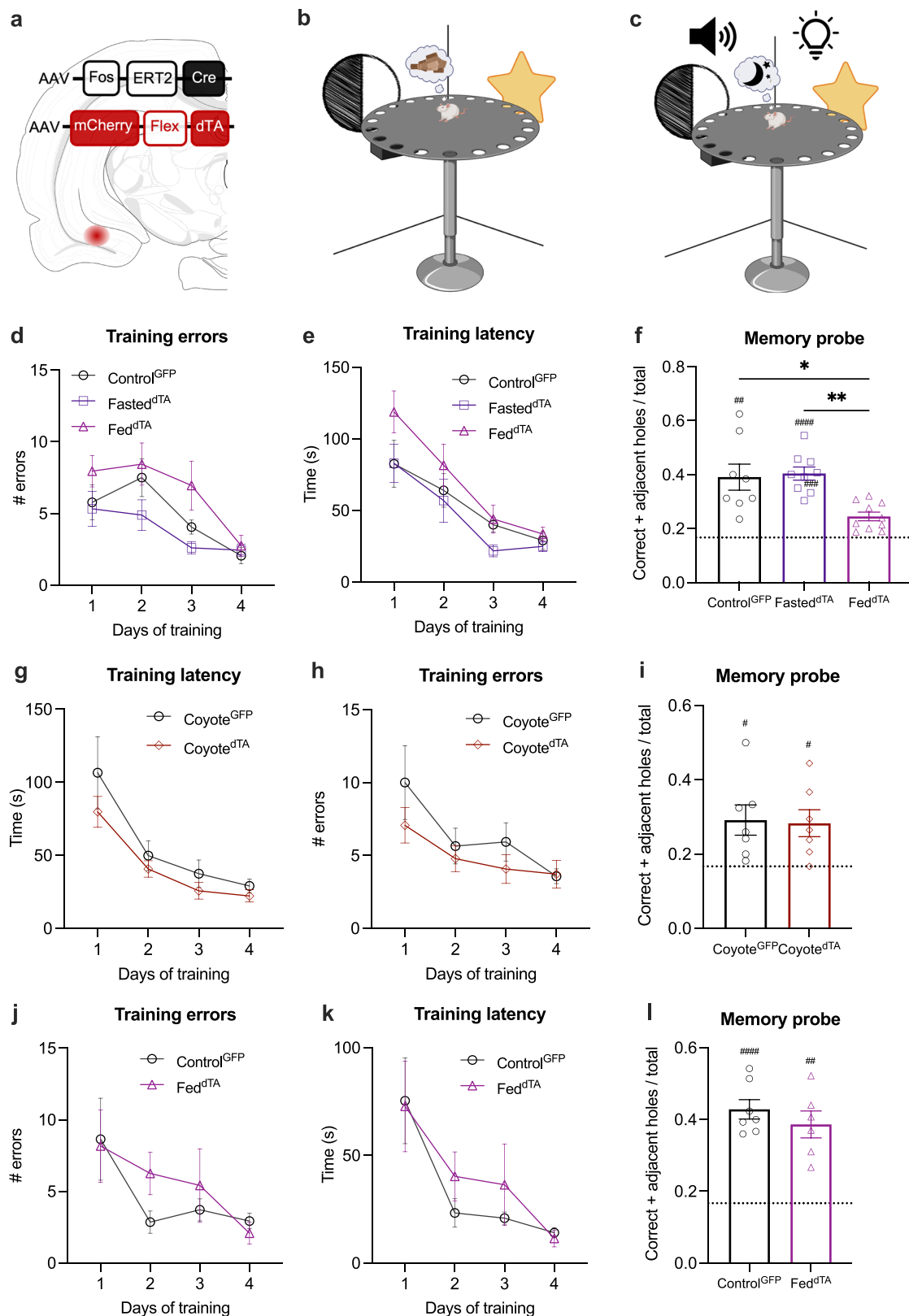


Fig. 1 | Dynamic elevations in ventral hippocampus calcium-dependent activity between eating bouts during meal consumption are predictive of performance during a foraging-related spatial memory task. **a** Diagram of viral approach for fiber photometry, adapted from the Brain Maps 4.0 structure of the rat brain⁷⁶. **b** Representative photomicrograph of viral expression and fiber placement in the ventral CA1 relative to the alveus (alv); scale bar 100 μ m (representative pattern was observed in all animals used in the analyses, $n = 5$). **c** Representative trace of a single animal of the increase in ventral CA1 calcium-dependent activity during the interbout intervals (purple). **d** Average change in z-score for fluorescence over the course of an eating bout versus an interval ($n = 5$ animals) ($p = 0.0341$). **e** Foraging-related spatial memory task apparatus (created in BioRender. Kanoski, S. (2025) <https://BioRender.com/5vog18n>). **f** Simple linear regression of the increase during interbout intervals predictive of subsequent performance in a separate foraging-

related spatial memory task. **g** Diagram of the viral approach for 4OHT-inducible expression of green fluorescent protein (GFP) in ventral CA1 neurons active in a Fasted or Fed state, adapted from the Brain Maps 4.0 structure of the rat brain⁷⁶. **h** Timeline for intraperitoneal (ip) injection of 4-hydroxitamoxifen (4OHT) under the Fasted, Fed or Coyote state. **i** Representative photomicrographs of the pyramidal layer of the ventral CA1 (CA1v(sp)) with GFP⁺ cell bodies from neurons that were active in the Fasted, Fed or Coyote state, relative to the alveus (alv); scale bar 100 μ m. **j** Quantification of ventral CA1 cell bodies labeled with GFP using the TRAP method under the Fasted ($n = 5$), Fed ($n = 4$) or Coyote ($n = 5$) state (p value for Group = 0.0130; p value for Fasted^{GFP} vs. Fed^{GFP} = 0.0120). Data are presented as mean \pm SEM. For Fig. 1d, two-tailed paired t-test ($n = 5$). For Fig. 1j, one-way ANOVA, Tukey post hoc $*p < 0.05$. No symbol indicates lack of significance.



differences in either the progressive ratio test (Extended Data Fig. 2o) or the time spent in the open areas of the zero maze (Extended Data Fig. 2p). Collectively, CA1v meal-responsive neurons appear to selectively modulate spatial memory for meal location without altering spatial memory in general, sucrose motivation, energy balance, or anxiety-like behavior.

Ventral hippocampus meal engram-encoding neurons project to the lateral hypothalamic area

To determine whether HPCv neurons engaged by meal consumption or fasting present distinct neural projection profiles, whole forebrain GFP⁺ axonal density was assessed in the brains of rats following 4OHT-induced GFP expression in CA1v neurons engaged under a Fasted

Fig. 2 | Ablation of ventral hippocampus meal-responsive neurons selectively impairs foraging-related spatial memory. **a** Diagram of viral approach for 4-hydroxytamoxifen (4OHT)-inducible Cre-dependent expression of diptheria toxin (dTA) (Fasted^{dTA} and Fed^{dTA}) or green fluorescent protein (Control^{GFP}) in ventral CA1 neurons active in the Fasted or Fed state, adapted from the Brain Maps 4.0 structure of the rat brain⁷⁶. **b** Diagram of Barnes maze apparatus for the foraging-related spatial memory task for the Control^{GFP} vs Fasted^{dTA} vs Fed^{dTA} groups (created in BioRender. Kanoski, S. (2025) <https://BioRender.com/5vog18n>). **c** Diagram of Barnes maze apparatus for the escape-based spatial memory task for the Control^{GFP} vs Fed^{dTA} groups (created in BioRender. Kanoski, S. (2025) <https://BioRender.com/ani3u4u>). **d** Average number of errors and **e** latency to find the food during training for the foraging-related spatial memory task for the Control^{GFP} ($n = 8$) vs Fasted^{dTA} ($n = 9$) vs Fed^{dTA} ($n = 10$) groups. **f** Performance index during the probe for the foraging-related spatial memory task for the Control^{GFP} ($n = 8$) vs Fasted^{dTA} ($n = 9$) vs Fed^{dTA} ($n = 10$) groups (p value for Group = 0.0009; p value for Control^{GFP} vs. Fed^{dTA} = 0.0239; p value for Fasted^{dTA} vs. Fed^{dTA} = 0.0011; p value for

1-sample t-test for Control^{GFP} = 0.0023; p value for 1-sample t-test for Fasted^{dTA} < 0.0001; p value for 1-sample t-test for Fed^{dTA} = 0.0009). **g** Average number of errors and **h** latency to find the food during training for the foraging-related spatial memory task for the Coyote^{GFP} ($n = 7$) vs Coyote^{dTA} ($n = 7$) groups. **i** Performance index during the probe for the foraging-related spatial memory task for the Coyote^{GFP} ($n = 7$) vs Coyote^{dTA} ($n = 7$) groups (p value for 1-sample t-test for Coyote^{GFP} = 0.0225; p value for 1-sample t-test for Coyote^{dTA} = 0.0183). **j** Average number of errors and **k** latency to find the escape box during training for the escape-based spatial memory task for the Control^{GFP} ($n = 7$) vs Fed^{dTA} ($n = 6$) groups. **l** Performance index during the probe for the escape-based spatial memory task for the Fed^{GFP} ($n = 7$) vs Fed^{dTA} ($n = 6$) groups (p value for 1-sample t-test for Control^{GFP} < 0.0001; p value for 1-sample t-test for Fed^{dTA} = 0.0020). Data are presented as mean \pm SEM. For **d**, **e**, **g**, **h** and **j**, **k**, two-way ANOVA. For **f**, Kruskal-Wallis, multiple comparisons. For **i** and **l**, two-tailed unpaired t-test; * p < 0.05, ** p < 0.01. For **f**, **i** and **l**, one-sample t-test, different from chance set at 0.1667; # p < 0.05, ## p < 0.01, ### p < 0.005, #### p < 0.001. No symbol indicates lack of significance.

(Fasted^{GFP}) or Fed (Fed^{GFP}) state. While GFP⁺ axonal projections were observed in the nucleus accumbens (ACB) and lateral septum (LS) of rats from both the Fasted^{GFP} and Fed^{GFP} groups (Fig. 3a, b), the presence of dense GFP⁺ axonal projections in the lateral hypothalamic area (LHA) was exclusive to Fed^{GFP} animals (Fig. 3c). In contrast, minimal GFP⁺ axonal density was observed in other known projection targets of CA1v neurons, including the prefrontal cortex (PFC), bed of the stria terminalis (BST), and amygdala (AMY) in either the Fasted^{GFP} or Fed^{GFP} groups (Extended Data Fig. 3a-c).

CA1v projections to the LS have also been linked with appetitive spatial memory³¹. To further validate that the CA1v-to-LHA pathway is preferentially recruited following meal consumption relative LS projections, AAV-retrograde tracers were injected into the LS (GFP) and LHA (mCherry) of rats (Fig. 3d) and brains were perfused following meal consumption for cFos immunostaining of CA1v meal-responsive neurons. Although a similar number of LS (GFP) and LHA-projecting (mCherry) CA1v neurons were labeled (Fig. 3e), only a limited amount of CA1v neurons expressed both GFP and mCherry (Fig. 3e), indicating that CA1v-to-LHA-projecting neurons have minimal collateral projections to LS. Further, while only a small proportion of LS-projecting CA1v neurons expressed cFos following meal consumption, the majority (~65%) LHA-projecting CA1v neurons were meal-responsive (Fig. 3g, h).

To determine whether LHA-projecting CA1v neurons are active during meal interbout intervals when animals are likely to encode meal engrams, we employed a dual-virus approach to express the calcium indicator GCaMP7s in HPCv neurons projecting to the LHA (Fig. 4a, b) and assessed bulk calcium-dependent activity time-stamped to behavioral events (active eating vs. inter-bout intervals) over the course of a 30 min meal following a 24 h fasting period. Results revealed that bulk calcium-dependent activity in CA1v neurons projecting to the LHA dynamically decreases during active eating bouts and increases during inter-bout intervals (Fig. 4c, d). To verify if these increases in calcium activity serve to encode foraging-related spatial information, we next employed a similar dual-virus approach to chemogenetically inhibit CA1v neurons sending projections to the LHA following lateral ventricle (LV) infusion of the chemogenetic ligand clozapine-N-oxide (CNO; 18 mmol) (Fig. 4e, f). In the absence of LV infusion, rats assigned to the vehicle (VEH) and CNO treatments presented similar number of errors and latencies to reach the food source throughout training (Fig. 4g, h). During the memory probe, rats receiving LV infusion of CNO failed to demonstrate a preference for the hole with the tunnel previously containing food and performed significantly worse than those receiving VEH (Fig. 4i and Extended Data Fig. 4a). LV infusion of CNO did not affect the total number of investigations performed nor the total distance traveled (Extended Data Fig. 4b, c). We have previously shown that LV infusion of CNO in the absence of hM4Di receptors does not impact performance in this task³¹. Thus, CA1v meal-

responsive neurons promote foraging-related spatial memory through a CA1v-to-LHA signaling pathway.

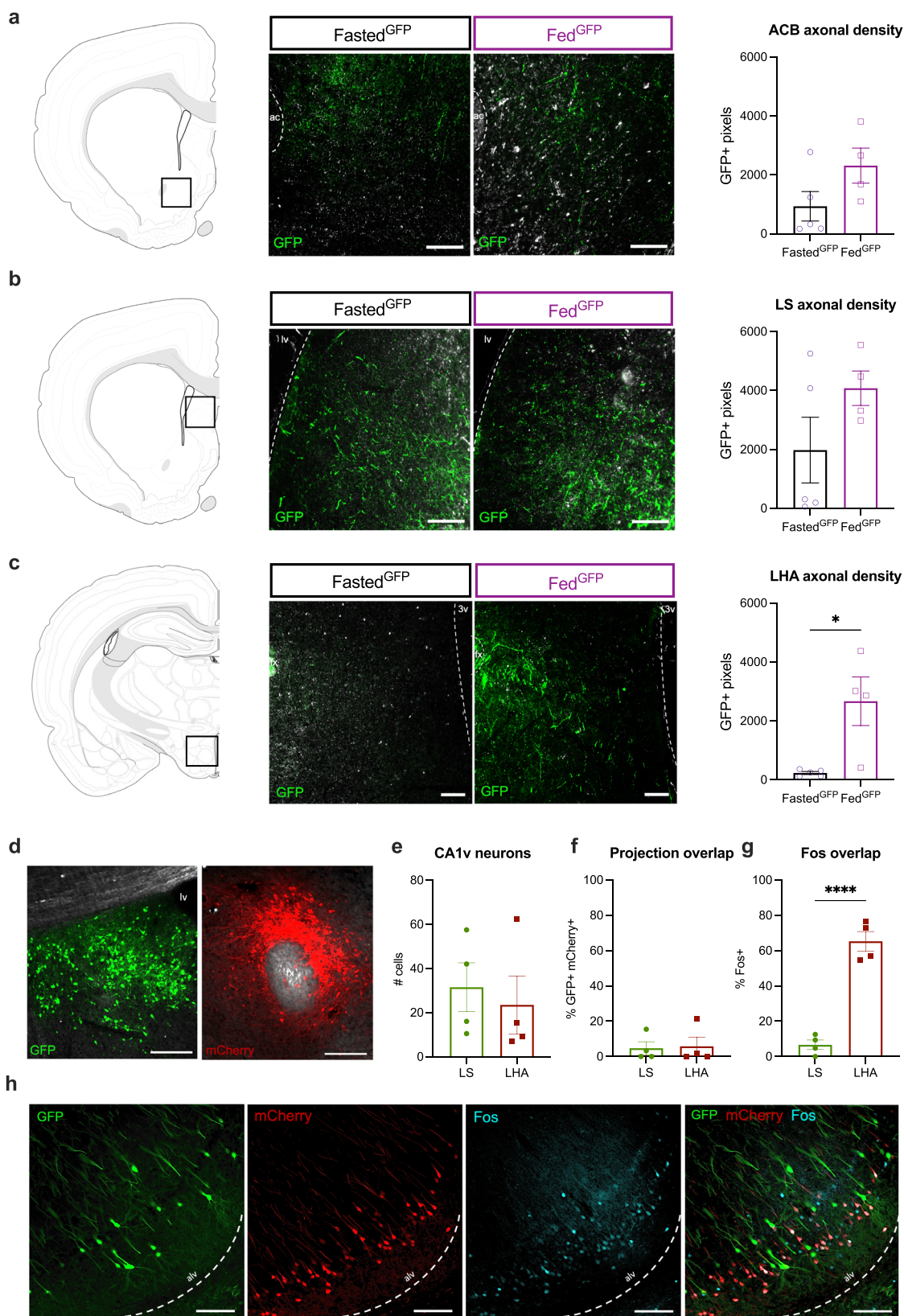
Ventral hippocampus serotonin type 2a receptor (5HT2aR) signaling is required for meal location memory

To identify a molecular signature that distinguishes HPCv meal-responsive neurons from fast-responsive neurons, we performed single nucleus RNA sequencing (snRNAseq) on HPCv microdissections obtained from rats under a Fasted or Fed state. After quality controls, the transcriptome profile of 38,138 nuclei were used to identify 17 cellular subtypes, identified by the expression of prototypical marker genes (Fig. 5a, b). We identified 1,615 cell type-specific differentially expressed genes (Fig. 5c, Supplemental Table 1 and 2), with neuronal transcriptome alterations overrepresented in a small number of cellular subtypes, with endothelial cells (cluster 15; 44 genes downregulated, 301 upregulated) and a population of CA1v excitatory neurons (cluster 5; 224 downregulated, 161 upregulated) undergoing the greatest changes upon meal consumption (Fig. 5d, Supplemental Table 1 and 2). Examining marker genes for cFos positive cells in the Fed and Fasted state (Supplemental Table 3), we identified an enrichment of *Htr2a* expression amongst the cFos positive cells in the Fed relative to Fasted state (Fig. 5e). This enrichment in *Htr2a* was confirmed via fluorescent in situ hybridization, with greater colocalization of cFos with *Htr2a* mRNA observed in the CA1v of rats perfused under a Fed state relative to those perfused under a Fasted state (Fig. 6a, b).

To assess the functional relevance of HPCv 5HT2aR signaling in meal-related memory, rats were bilaterally implanted with cannulae targeting the CA1v for infusion of the selective 5HT2aR antagonist MI00907 (1 μ g/hemisphere; M3324, Sigma-Aldrich) or its vehicle (VEH) (Fig. 6c). Rats were trained in the foraging-related spatial memory task and, in the absence of infusions, both groups presented similar number of errors and latencies to reach the food source throughout training (Fig. 6d, e). At the memory probe, rats receiving MI00907 failed to demonstrate a preference for the hole previously associated with meal consumption and performed significantly worse than animals receiving VEH (Fig. 6f and Extended Data Fig. 5a), an observation analogous to the effect of chemogenetically silencing CA1v to LHA projections. This impairment was not associated with differences in the total number of investigations or distance traveled at the time of the probe (Extended Data Fig. 5b, c). These data suggest that HPCv meal-responsive neurons mediate their effects on foraging-related spatial memory via 5HT2aR signaling.

Ventral hippocampus meal-responsive neurons dictate the temporal interval between meals

Episodic memory for meal consumption not only includes information about spatial and contextual cues that inform about the location of the meal, but also temporal information regarding when the meal was



consumed. The latter powerfully influences meal timing and amount consumed in both humans and rodent models in a manner indicating that enhanced memory for when a recent meal was consumed extends the timing to begin the next spontaneous/voluntary meal (i.e., longer inter-meal interval), whereas impaired memory for a recent meal shortens the timing until the next meal (i.e., shorter inter-meal

interval)^{15,6,15,16,36}. To determine whether acute manipulation of signaling pathways from CA1v meal-responsive neurons influences food intake and meal timing, meal pattern analyses were conducted following either CA1v 5HT2aR antagonism or CA1v-to-LHA chemogenetic silencing prior to dark onset in free-feeding animals. CA1v infusion of the 5HT2aR antagonist M100907 increased food intake relative to VEH

Fig. 3 | Ventral hippocampus meal-responsive neurons project to the lateral hypothalamic area. **a** *Left*: Diagram of a coronal section of the nucleus accumbens (ACB), adapted from the Brain Maps 4.0 structure of the rat brain⁷⁶. *Middle*: Representative photomicrographs of axonal green fluorescent protein (GFP) expression in the ACB from ventral CA1 neurons active in the Fasted (Fasted^{GFP}) ($n = 5$) or Fed (Fed^{GFP}) ($n = 4$) state, relative to the anterior commissure (ac); scale bar 100 μm . *Right*: Average number of GFP⁺ pixels in the ACB. **b** *Left*: Diagram of a coronal section of the lateral septum (LS), adapted from the Brain Maps 4.0 structure of the rat brain⁷⁶. *Middle*: Representative photomicrographs of axonal GFP⁺ expression in the LS from ventral CA1 neurons active in the Fasted (Fasted^{GFP}) ($n = 5$) or Fed (Fed^{GFP}) ($n = 4$) state, relative to the lateral ventricle (lv); scale bar 100 μm . *Right*: Average number of GFP⁺ pixels in the LS. **c** *Left*: Diagram of a coronal section of the lateral hypothalamic area (LHA), adapted from the Brain Maps 4.0 structure of the rat brain⁷⁶. *Middle*: Representative photomicrographs of axonal GFP⁺ expression in the LHA from ventral CA1 neurons active in the Fasted (Fasted^{GFP})

($n = 5$) or Fed (Fed^{GFP}) ($n = 4$) state, relative to the fornix (fx) and 3rd ventricle (3 v); scale bar 100 μm . *Right*: Average number of GFP⁺ pixels in the LHA (p value = 0.0159). **d** *Left*: Representative photomicrograph of retrograde GFP viral expression in the LS, relative to the lv; scale bar 200 μm . *Right*: Representative photomicrograph of retrograde mCherry viral expression in the LHA, relative to the fx; scale bar 200 μm . **e** Average number of LS (GFP) ($n = 4$) and LHA (mCherry) ($n = 4$)-projecting neurons labeled in the CA1v. **f** Average percentage of CA1v neurons sending axonal projections to both the LS (GFP) ($n = 4$) and LHA (mCherry) ($n = 4$). **g** Average percentage of LS (GFP) ($n = 4$) and LHA (mCherry) ($n = 4$)-projecting CA1v neurons expressing cFos in the Fed state (p value < 0.0001). **h** Representative photomicrograph of fluorescent in situ hybridization for *Fos* (cyan) in LS (GFP) and LHA (mCherry)-projecting neurons of the CA1v, relative to the alveus (alv); scale bar 100 μm . Data are presented as mean \pm SEM. For **a–c** and **d–g**, two-tailed unpaired t -test; * $p < 0.05$, **** $p < 0.0001$. No symbol indicates lack of significance.

at the 2 h timepoint (Fig. 7a), and while no statistically significant differences were detected in either meal size (Fig. 7b) or meal frequency (Fig. 7c), inter-meal intervals were decreased/shorter by CA1v 5HT2aR antagonism (Fig. 7d), an outcome consistent with impaired memory for the timing of recently consumed meals. Similarly, LV infusion of CNO to disconnect CA1v-to-LHA signaling increased food intake relative to VEH treatment over a period of 6 h (Fig. 7e) and, while no changes were observed in meal size (Fig. 7f), this effect was driven by an increase in meal frequency (Fig. 7g) and a decrease in inter-meal intervals (Fig. 7h). The timing of these effects was specific to each separate drug treatment as CA1v 5HT2aR antagonism did not significantly impact food intake and meal patterns over a period of 6 h (Extended Data Fig. 7a–d) and LV infusion of CNO failed to alter food intake and meal patterns over a period of 2 h (Extended Data Fig. 7e–h). Together, these results highlight a role for HPCv meal-responsive neurons to encode both spatial and temporal aspects of meal-related memories, and that these processes influence spontaneous eating patterns.

Discussion

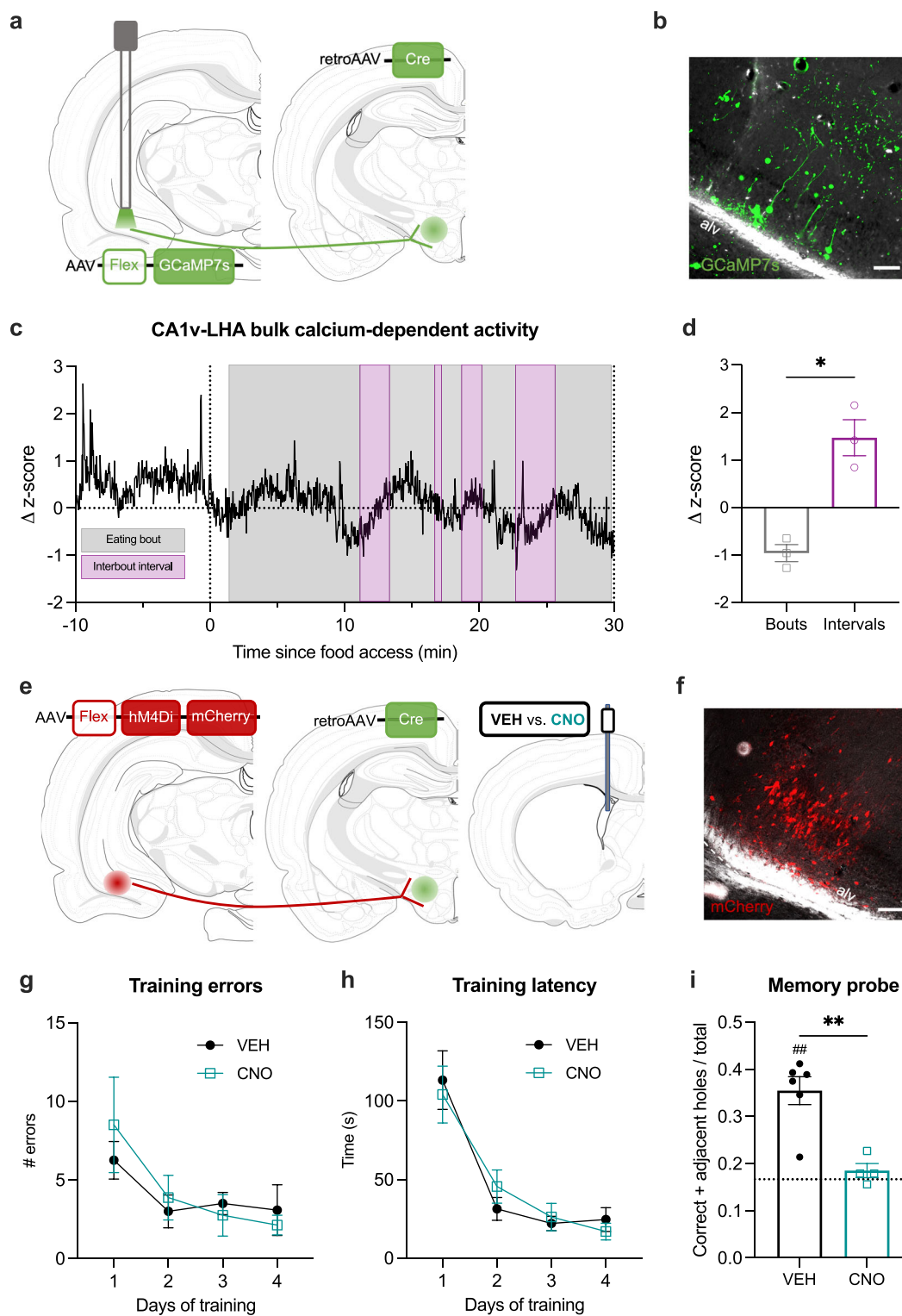
Memory function strongly contributes to the control of eating behavior, yet the neural substrates governing this phenomenon have been minimally investigated. Here, we show that activation of a population of hippocampal neurons (CA1v pyramidal) during meal consumption serves to encode meal-related spatial and temporal mnemonic information. We functionally, molecularly, and anatomically characterize these meal-responsive neurons and demonstrate that they project to the lateral hypothalamic area (LHA) and express the 5HT2a receptor. This neuronal ensemble selectively mediates meal-related memory encoding without influencing food motivation or other analogous memory processes not related to meal consumption, and further, dictates the temporal sequence of spontaneous meal initiation. Together, these findings provide evidence for the formation of meal engrams in the CA1v that serve to facilitate foraging behavior, and when food is readily available, the temporal parameters of meal consumption.

That HPCv neurons are engaged upon food consumption is consistent with previous studies revealing that optogenetic inhibition of HPCv neurons influences food intake^{35,36,34}. Further, fiber photometry recordings of HPCv calcium-dependent activity reveal dynamic changes during foraging and food-seeking behaviors^{31,33}. Our present results advance these findings by establishing a role for HPCv neuronal activity during eating behaviors in encoding meal-related memory, thus providing a mechanistic framework for this previous literature. Further, HPCv calcium activity dynamics during meal consumption reveal elevations selectively during the intervals between active eating bouts. This suggests that HPCv neurons more effectively encode meal-associated memories during periods of a meal when animals are rearing or exploring and thus can more easily observe exteroceptive

features of the eating environment. Future work is needed to determine whether these neurons respond selectively to nutritive signals, visuospatial cues during meal consumption, or a combination of the two.

The CA1v regulates eating behaviors through diverse neuronal pathways, including axonal projections targeting the LS^{33,34}, ACB^{13,37}, and PFC³⁸. Our findings reveal that CA1v meal-responsive neurons predominantly send axonal projections to the LHA, which is in line with the well-known contribution of the LHA in regulating eating behaviors³⁹. We have previously shown that CA1v neurons also communicate via a multi-synaptic pathway to the LHA via the LS, and that this pathway influences appetitive spatial memory without influencing food intake or the temporal intervals between meals³¹. That direct and second-order projections from the CA1v to the LHA promote appetitive mnemonic processes, yet only a direct LHA connection influences food intake and meal patterns, suggests that hippocampal-hypothalamic direct and indirect pathways function on both convergent and different processes governing energy balance. Consistent with this framework, previous work identified a role for direct CA1v-to-LHA neuronal projections in modulating appetite and meal parameters through ghrelin signaling^{11,14}. Therefore, it may be the case that peri-prandial concentrations of ghrelin recruit CA1v meal-responsive neurons to encode mnemonic information, which is consistent with findings that hippocampus ghrelin signaling promotes hippocampal neuronal plasticity and conditioned cue-potentiated overeating^{10,40}. Another relevant recent study reported that neurons of the ventral subiculum, a region adjacent to the hippocampus proper, that project to the nucleus accumbens (ACB) are recruited during food anticipatory behavior in a ghrelin-sensitive manner, whereas ventral subiculum neurons projecting to the LHA respond to the presentation of salient stimuli⁴¹. Whether these ventral subiculum projections work in concert with CA1v meal-responsive neurons to encode meal-related memories represents an intriguing follow-up direction.

Present results identify the HPCv as a site of action for serotonin's influence on food intake-related processes. The predominance of the literature on serotonin signaling and food intake control focuses on the anorexigenic effects of the serotonin type 2c receptor (5HT2cR), notably in the hindbrain^{42–44}. Here, we show a role for HPCv 5HT2aR in modulating food intake, which is consistent with reports of *Htr2a* variants influencing food intake and preferences in humans^{45,46}. In rodents, 5HT2aR-expressing neurons in the central amygdala are responsive to fasting and modulate food consumption^{47,48}. That HPCv 5HT2aR signaling influences food intake through memory function is in line with reports in humans with *Htr2a* allele variants influencing hippocampal function^{49–51} and work in rodents illustrating a role for 5HT2aR signaling in learning in memory processes^{52–57}, and specifically in the HPCv⁵⁸. In rats, the caudal region of the dorsal raphe nucleus (DRN) serves as the source of serotonin to the HPCv^{59,60}. Given that food consumption increases the activity of DRN serotonin neurons^{61,62} and that 5HT2aR agonism triggers neural



excitation in hippocampal neurons⁵⁵, one possibility is that meal-induced serotonin release by DRN neurons acts within the CA1v to recruit meal-responsive neurons and facilitate meal engram formation. Our work identifies a mechanism through which 5HT_{2a}R signaling in HPCv meal-responsive neurons influences eating behaviors by encoding meal-related memory.

In addition to 5HT_{2a}R, dopamine receptors are also expressed in the hippocampus, and hippocampal dopamine receptor binding is elevated following nutrient consumption in humans⁶³. In mice,

activation of dopamine receptor type 2-expressing neurons of the dorsal subregion of the hippocampus both reduces food intake and disrupts the encoding of contextual food-related memory⁶⁴. Whether dopamine receptor signaling in the HPCv subregion is also relevant to food intake and meal-related memory, and whether dopamine receptor and 5HT_{2a}R systems functionally interact in the hippocampus, requires further evaluation.

Memories relating to the timing of a meal and the amount of food consumed potentially influence subsequent hunger, satiety, and caloric

Fig. 4 | Ventral hippocampus neurons projecting to the lateral hypothalamic area increase activity between eating bouts and promote foraging-related spatial memory. **a** Diagram of viral approach for expression of GCaMP7s in ventral CA1 neurons projecting to the lateral hypothalamic area and implantation of the optic fiber, adapted from the Brain Maps 4.0 structure of the rat brain⁷⁶. **b** Representative photomicrograph of GCaMP7s expression for placement validation of viral injections, relative to the alveus (alv); scale bar 100 μm (representative pattern was observed in all animals used in the analyses, *n* = 3). **c** Representative trace of a single animal of the increase in calcium-dependent activity during the interbout intervals (purple) in ventral hippocampus neurons projecting to the lateral hypothalamic area. **d** Average change in z-score for fluorescence over the course of an eating bout versus during an interbout interval (*n* = 3 animals) (*p* value = 0.0165). **e** Diagram of viral approach for expression of hM4Di receptors in ventral CA1 neurons projecting to the lateral hypothalamic area and administration

of vehicle (VEH) or clozapine-N-oxide (CNO) through a lateral ventricle (LV) canula, adapted from the Brain Maps 4.0 structure of the rat brain⁷⁶. **f** Representative photomicrograph of mCherry expression for placement validation of viral injections, relative to the alveus (alv); scale bar 100 μm (representative pattern was observed in all animals used in the analyses, *n* = 10). **g** Average number of errors and **h** latency to find the food during training for the foraging-related spatial memory task in animals assigned to VEH (*n* = 6) or CNO (*n* = 4) groups. **i** Performance index during the probe for the foraging-related spatial memory task, 1 h following LV administration of VEH (*n* = 6) or CNO (*n* = 4) (Group comparison *p* value = 0.0024; *p* value for 1-sample t-test = 0.0014 for VEH group). Data are presented as mean ± SEM. For **d**, two-tailed paired t-test. For **g–h**, two-way ANOVA. For **i**, two-tailed unpaired t-test (*n* = 4–6/group); **p* < 0.05, ***p* < 0.01. For **i**, one-sample t-test, different from chance set at 0.1667; ##*p* < 0.01. No symbol indicates lack of significance.

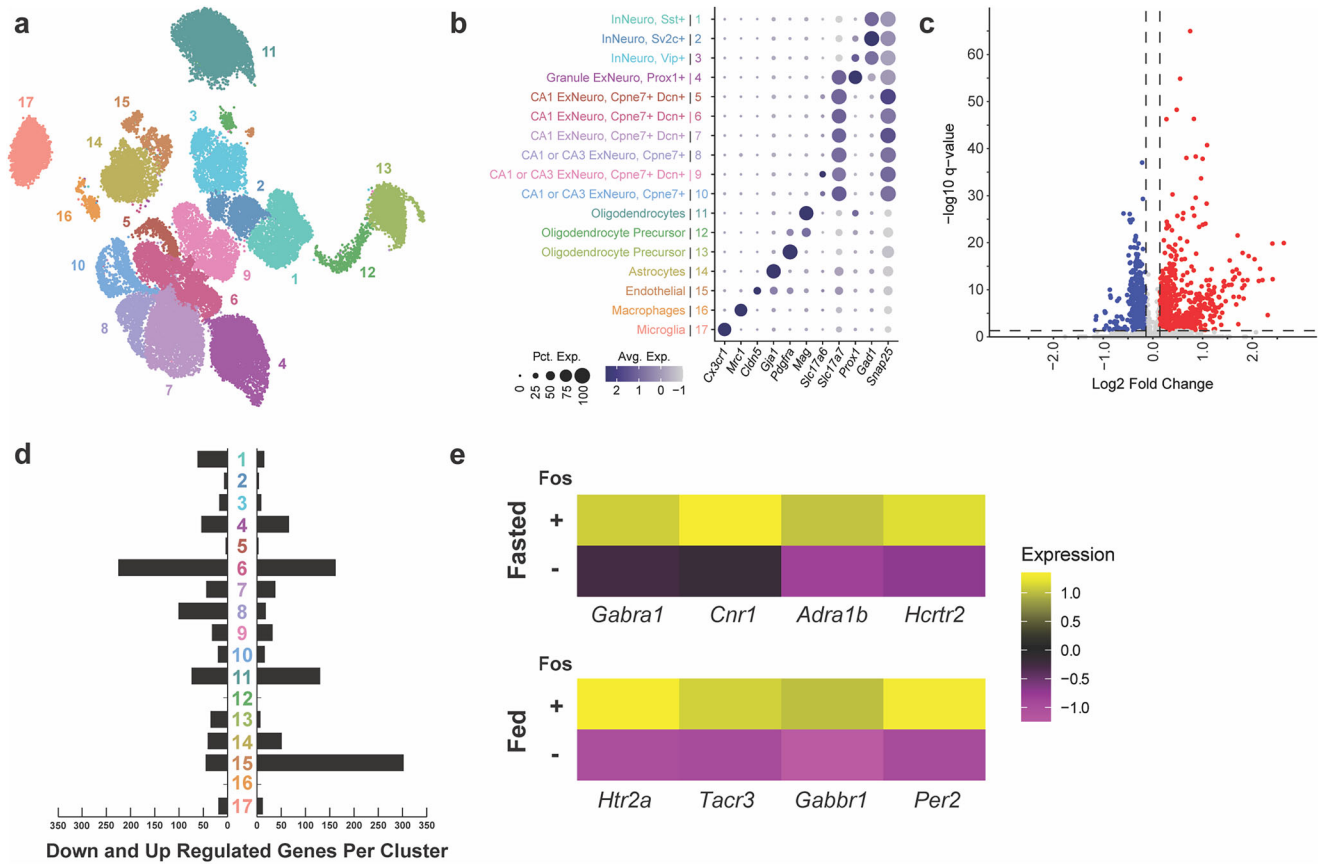


Fig. 5 | Meal consumption alters the transcriptional profile of ventral hippocampus endothelial cells and CA1v excitatory neurons and engages SHT2aR expressing cells. **a** Uniform manifold approximation and projection (UMAP) of the ventral hippocampus (HPCv) samples identifying 17 clusters. **b** Annotation of cellular subtypes with known makers of HPCv cellular subtypes. The size and color of dots are proportional to the percentage of cells expressing the gene (Pct. Exp) and the average expression levels of the gene (Avg. Exp.), respectively. The cluster

numbers and colors are matched to that of the UMAP. **c** Volcano plot depicting the number of significant differential expression events induced by meal consumption (Wilcoxon rank sum test, bonferroni correction; *p* values adjusted for multiple testing). **d** Number of genes with meal consumption-altered increased (right) or decreased (left) expression per cluster. **e** Heatmaps of select genes enriched in *Fos*-cells under a Fasted or Fed state.

consumption^{1–4}. These phenomena are strikingly illustrated in patients suffering from medial temporal lobe damage who are unable to form new episodic memories and will thus, if permitted, consume multiple consecutive meals in a short temporal window, resulting in greater overall intake⁶⁵. Additionally, human obesity and disordered eating behaviors are associated with alterations within an orexigenic hippocampal subnetwork⁸. Our present findings illuminate the neural circuitry mediating these effects as both chemogenetic inhibition of a CA1v-to-LHA signaling pathway and HPCv 5HT2aR antagonism disrupted meal-related memory, increased caloric intake, and shortened the inter-meal temporal window, an effect also consistent with rodent

studies demonstrating effects of HPCv neuronal inhibition on subsequent meal patterns^{15,16,36}. These effects were evaluated under conditions of standard chow consumption, whereas memory evaluation procedures for meal location utilized sucrose consumption. Given that dietary fat and sugar can be sensed by the brain via divergent pathways^{66,67}, further research could explore whether CA1v neurons encode meal-related memories in a macronutrient-dependent manner. Based on evidence from both humans and rodent models, degraded memories for a recent meal can yield two outcomes: (1) A reduced latency to initiate the next voluntary meal (i.e., increased meal frequency), and (2) Increased size of a subsequent meal⁵. Our present

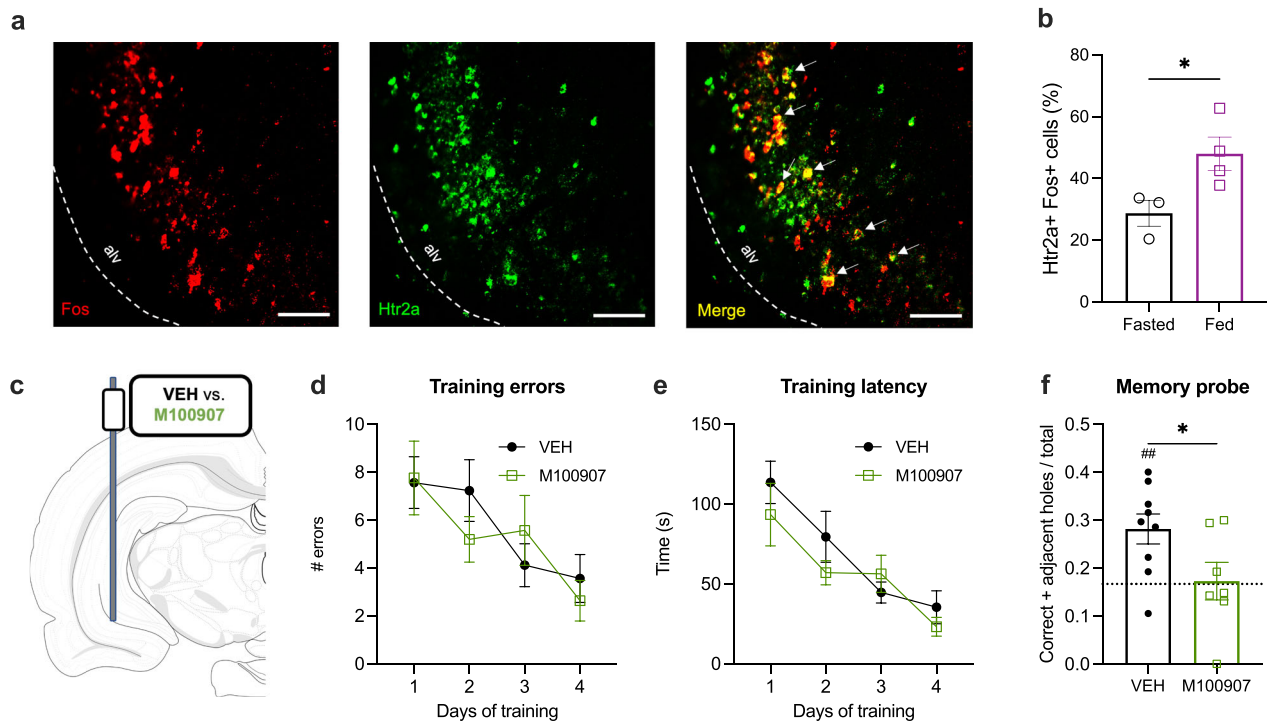


Fig. 6 | Ventral hippocampus 5HT_{2A}R expressing neurons are engaged by a meal, project to the lateral hypothalamic area, and are functionally required for foraging-related spatial memory. **a** Representative photomicrograph of fluorescent in situ hybridization for *Fos* (red) and *Htr2a* (green) in the ventral CA1, relative to the alveus (alv); scale bar 100 μ m. **b** Percentage of ventral CA1 *Fos*⁺ cells that co-express *Htr2a* in rats perfused under a Fasted ($n=3$) or Fed state ($n=4$) (p value = 0.0463). **c** Diagram of approach for ventral CA1 administration of vehicle (VEH) or the 5HT_{2A}R antagonist M100907 (1 g/hemisphere), adapted from the Brain Maps 4.0 structure of the rat brain⁷⁶. **d** Average number of errors and

e latency to find food during the training for the foraging-related spatial memory task for animals assigned to group VEH ($n=9$) or M100907 ($n=7$). **f** Performance during the probe for the foraging-related spatial memory task, 5 min following ventral CA1 infusion of VEH ($n=9$) or M100907 ($n=7$) (Group comparison p value = 0.0453; p value for 1-sample t-test = 0.0064 for Group VEH). Data are presented as mean \pm SEM. For **b**, **f**, two-tailed unpaired t-test. For **d**, **e**, two-way ANOVA; * $p < 0.05$. For **f**, one-sample t-test, different from chance set at 0.1667; ## $p < 0.01$. No symbol indicates lack of significance.

results expand these findings by revealing that acute vs. chronic disruption of meal memory circuitry may differentially impact these outcomes. For example, acute disruption of this circuitry, via either silencing of CA1v-LHA communication or CA1v 5HT_{2A}R blockade, reduced the latency between meals without significantly impacting meal size. On the other hand, chronic disruption of this circuitry, via diphtheria toxin TRAP-mediated ablation of meal-responsive CA1v neurons, yielded an increase in average meal size, along with a compensatory reduction in meal frequency. It is unknown how acute or chronic disruption of meal memory circuitry would influence eating patterns under conditions where food is not freely available, and thus, where effort-based foraging is required for survival. We hypothesize that under such conditions, chronic disruption of this circuit would lead to overall hyperphagia, as was observed with our two models of acute circuit disruption.

Present results should be interpreted in the context of a few limitations. For example, the TRAP-mediated ablation experiment employs a chronic loss of function approach that may lead to compensatory neural adaptations secondary to the loss of CA1v responsive neurons. Therefore, different outcomes might be observed with an activity-based acute and reversible inhibitory approach, a notion consistent with data from our meal patterns analysis in which chronic loss of CA1v meal-responsive neurons fails to affect caloric intake whereas either reversible chemogenetic inhibition of CA1v-to-LHA projections or CA1v 5HT_{2A}R blockade increased food intake. Additionally, despite being driven by activity-based neuroanatomical tracing and snRNAseq experiments, our CA1v-to-LHA chemogenetic and 5HT_{2A}R pharmacology approaches are not restricted to HPCv meal-

responsive neurons and their impact on other forms of spatial memory has not been assessed. Nonetheless, these findings provide a neural systems mechanism through which learning and memory processes synergize with eating behaviors.

Results from our snRNAseq of meal-responsive CA1v neurons open the door to promising new research avenues. For example, future work should explore the function of differentially expressed genes in discrete neural populations of the HPCv in response to meal consumption. Results (sequencing dataset publicly available) reveal that the largest number of differentially expressed genes are present in a cell cluster delineated by the presence of endothelial cells, which comprise the blood-brain barrier. Whether the blood-brain-barrier undergoes permeability changes to facilitate HPCv function upon meal consumption is an exciting area to investigate. Given that the majority of differentially expressed genes in this cluster were up-regulated in the Fed vs. Fasted state, it may be that blood-brain barrier permeability is increased during and immediately after a meal to preclude blood-to-brain entry of potential toxins introduced from the food consumed. Another question arises with regards to the status of these HPCv meal-responsive neurons in the context of obesity and whether they can be targeted to reduce food intake in a diet-induced obese model. Answering these questions would significantly advance our understanding of the neurobiology underlying the higher-order control of eating behavior. Overall, this work identifies a population of HPCv neurons that is enriched in 5HT_{2A}R and projects to the LHA to encode the engram for meals. Importantly, these findings have direct translational relevance, as human obesity and disordered eating behaviors are associated with alterations

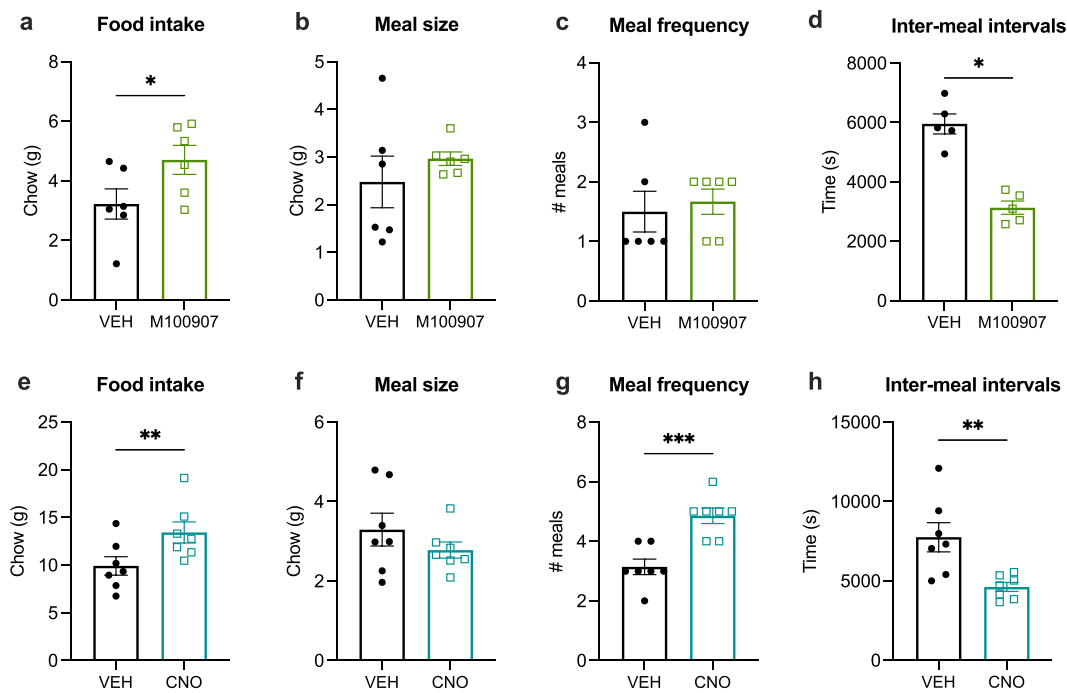


Fig. 7 | Blockade of ventral hippocampus to lateral hypothalamic area signaling or 5HT_{2a}R signaling increases food intake by reducing temporal intervals between meals during spontaneous feeding. **a** Average 2 h chow intake ($p = 0.0290$), **b** meal size, **c** meal frequency and **d** inter-meal intervals following ventral CA1 administration of vehicle (VEH) ($n = 6$) or M100907 ($n = 6$) ($p = 0.0171$). **e** Average 6 h chow intake ($p = 0.0052$), **f** meal size, **g** meal frequency ($p = 0.0010$),

and **h** inter-meal intervals following lateral ventricle administration of vehicle (VEH) ($n = 7$) or clozapine-N-oxide (CNO) ($n = 7$) ($p = 0.0081$) in rats expressing hM4Di receptors in ventral CA1 neurons projecting to the lateral hypothalamic area. Data are presented as mean \pm SEM. Two-tailed paired t-test; * $p < 0.05$, ** $p < 0.01$, *** $p < 0.001$. No symbol indicates lack of significance.

within a hippocampal subnetwork with functional connectivity to the LHA⁸.

Methods

Animals

Adult male Sprague–Dawley rats (Envigo; 250–275 g on arrival) were individually housed with *ad libitum* access to water and chow (LabDiet 5001, LabDiet, St. Louis, MO) on a 12 h:12 h reverse light/dark cycle. All procedures were approved by the University of Southern California Institute of Animal Care and Use Committee.

Intracranial injections

Rats were anesthetized via an intramuscular injection of an anesthesia cocktail (ketamine 90 mg/kg body weight [BW], xylazine, 2.8 mg/kg BW and acepromazine and 0.72 mg/kg BW) followed by a pre-operative, subcutaneous injection of analgesic (buprenorphine SR, 0.65 mg/kg BW). Following shaving and preparation of the incision site with iodine and ethanol swabs, rats were placed in a stereotaxic apparatus for viral infusions using a microinfusion pump (Harvard Apparatus, Cambridge, USA) connected to a 33-gauge microsyringe injector attached to a PE20 catheter and Hamilton syringe at a flow rate of 83.3 nL/s. Injectors were left in place for 2 min post-injection, prior to placement of an indwelling cannula or closing of the incision site using skin adhesive.

Fiber photometry

To record bulk calcium-dependent activity in the ventral CA1 (CA1v), rats received bilateral infusion (300 nL/side) of a synapsin-driven GCaMP7s-expressing virus (AAV9-hSyn-GCaMP7s-WPRE; Addgene, Watertown, USA) at the following coordinates: -4.9 mm AP (defined at bregma), ± 4.8 mm ML (defined at bregma), and -7.8 mm (defined at skull surface at site). To record bulk calcium-dependent activity from

CA1v neurons projecting to the LHA, rats received bilateral infusion (300 nL/side) of a Cre-dependent synapsin-driven GCaMP7s-expressing virus (AAV9-hSyn-GCaMP7s-WPRE; Addgene, Watertown, USA) at the same coordinates as above, in addition to a bilateral LHA injection (200 nL/side) of a retrograde AAV expressing Cre recombinase (AAV2[retro]-hSYNI-EGFP-2A-iCre-WPRE; Vector BioLabs) at the following stereotaxic coordinates: -2.9 mm AP, ± 1.1 mm ML, and -8.6 mm DV (all defined at bregma). A fiber-optic cannula (Doric Lenses Inc, Quebec, Canada) was implanted at the injection site and affixed to the skull with jeweler's screws, instant adhesive glue, and dental cement.

Photometry recording sessions were conducted as described previously^{31,68}. Briefly, 24-h-fasted animals were placed in a familiar arena and were given access to chow pellets for 30 min, following a 15 min recording of baseline calcium-dependent activity. Photometry signal was acquired using the fiber photometry system (Neurophotometrics, San Diego, USA) at a sampling frequency of 40 Hz and administering alternating wavelengths of 470 nm (calcium-dependent) or 415 nm (calcium-independent). Active eating bouts were time-stamped in real-time by experimenters observing the animals using the data acquisition software Bonsai.

Photometry signal was corrected by subtracting the calcium-independent from the calcium-dependent signal fitting the result to a biexponential curve. This corrected fluorescence signal was normalized by calculating, for each rat, the $\Delta F/F$ using the average fluorescence signal for the entire recording and further converting it to z-scores.

Targeted recombination in active population (TRAP)

Rats received bilateral CA1v injection of a 1:1 cocktail of viruses (400 nL/side): [1] a tamoxifen-inducible virus expressing Cre recombinase under the control of a cFos promoter (AAV8-cFos-ERT2-Cre

ERT2-PEST; Stanford Vector Core, Stanford, USA) and [2] a Cre-dependent virus expressing green fluorescent protein (AAV1-pCAG-Flex-eGFP-WPRE; Addgene viral prep #51502-AAV1 gifted by Hongkui Zeng⁶⁹) or diphtheria toxin (AAV2/9-EF1a-mCherry-Flex-dTA; Neurophotronics, Quebec, Canada). Three weeks following surgery, 24 h fasted rats are offered 30 min access to chow pellets (Fed) or not (Fasted), 2 h prior to receiving an intraperitoneal (ip) injection of 4-hydroxytamoxifen (4OHT; 15 mg/kg; H6278, Sigma-Aldrich, St. Louis, USA) dissolved in saline with 2% Tween-80 and 5% DMSO, similarly to⁷⁰. Behavioral measures and histological analyses commenced at least 1 week following 4OHT-induced recombination.

For the histological analyses of GFP+ cell bodies and axonal projections, coronal sections were compared between rats undergoing 4OHT-driven expression of GFP (AAV8-cFos-ERT2-Cre-ERT2-PEST mixed with AAV-Flex-GFP) in the Fed (Fed^{GFP}) versus Fasted (Fasted^{GFP}) state. For the chronic ablation experiment, rats undergoing dTA-mediated ablation (AAV-8-cFos-ERT2-Cre-ERT2-PEST mixed with AAV2/9-EF1a-mCherry-Flex-dTA) induced by 4OHT administration following meal consumption (Fed^{dTA}) or not (Fasted^{dTA}) were compared to animals with CA1v GFP expression (AAV-8-cFos-ERT2-Cre-ERT2-PEST mixed with AAV-Flex-GFP) induced by 4OHT administration (Control^{GFP}).

For the exposure to coyote urine, rats received bilateral CA1v injections of a 1:1 cocktail of viruses (400 nL/side): [1] AAV8-cFos-ERT2-Cre-ERT2-PEST (Stanford Vector Core) and [2] AAV1-pCAG-Flex-GFP (Addgene viral prep #51502-AAV1) for the Coyote^{GFP} group or AAV2/9-EF1a-mCherry-Flex-dTA (Neurophotronics) for the Coyote^{dTA} group. Three weeks following surgery, all rats were fasted for 24 h and exposed to cups filled with coyote urine (Maine Outdoor Solutions LLC, Hermon, Maine, USA) placed 1 ft. away from the homecage for 30 min and received an ip injection of 4OHT (15 mg/kg; H6278, Sigma-Aldrich) 2 h later. Behavioral measures and histological analyses commenced at least 2 week following 4OHT-induced administration.

Foraging-related spatial memory task

The foraging-related spatial memory task was conducted as described previously³¹. Briefly, using an elevated circular platform with 18 equally distanced holes surrounding by visuospatial cues on the walls, rats were trained, over the course of 4 days (3 min/trial, 2 trial/day), to navigate towards the escape hole containing 5 sucrose pellets (F0023, Bio-Serv Flemington, USA). Distinct spatial cues are present on the walls surrounding the table and low-level ambient lighting is provided by floor lamps. Memory probe occurred 72 h after the last training session and consisted of a 2-min trial during which preference of the rat for the previously reinforced hole was assessed in the absence of sucrose pellets. A performance index was calculated by dividing the number of investigations for the previously reinforced hole and its adjacent holes by the total number of investigations. Investigations were quantified by tracking animal's head using the AnyMaze Behavior Tracking Software (Stoelting, Wood Dale, USA).

Escape-based spatial memory task

The escape-based spatial memory task was conducted as described previously³¹, using a protocol that is identical to the foraging-related spatial memory task, with the exception that sucrose pellets were absent, and a mildly aversive overhead bright light (120 W) and white noise (75 dB) were presented until the rat found the escape box.

Retrograde tracing

Rats received a unilateral injection (200 nL) of a retrograde AAV expressing GFP (AAVrg-CAG-GFP; Addgene viral prep # 37825-AAVrg gifted by Edward Boyden) into the LS at the following coordinates: +0.84 mm AP, + or -0.5 mm ML, and -4.8 mm DV (all defined at bregma). The same rats also received a unilateral injection (200 nL) of a retrograde AAV expressing mCherry (AAVrg-hSyn-mCherry; Addgene

viral prep # 11472-AAVrg gifted by Karl Deisseroth) into the LHA at the following coordinates: -2.9 mm AP, + or -1.1 mm ML, and -8.6 mm DV (all defined at bregma). Following a 2-week recovery period, rats were fasted for 24 h, offered a 30 min meal and perfused 90 min later for cFos immunostaining.

Chemogenetic silencing of the HPCv-lateral hypothalamic area (LHA) pathway

Chemogenetic silencing of CA1v projections to the LHA was performed using a previously published dual-viral approach³¹. Rats received bilateral HPCv injection (300 nL/side) of a Cre-dependent hM4Di-expressing virus (AAV2-Flex-hM4Di-mCherry; Addgene) using the same stereotaxic coordinates as the TRAP approach, as well as bilateral LHA injection (200 nL/side) of a retrograde AAV expressing Cre recombinase (AAV2[retro]-hSYNI-EGFP-2A-iCre-WPRE; Vector Bio-Labs) at the following stereotaxic coordinates: -2.9 mm AP, ±1.1 mm ML, and -8.6 mm DV (all defined at bregma). Animals were also implanted with a unilateral indwelling cannula (26-gauge, Plastics One, Roanoke, USA), affixed to the skull with jeweler's screws, instant adhesive glue and dental cement, targeting the lateral ventricle (LV) at the following stereotaxic coordinates: -0.9 mm AP (defined at bregma), +1.8 mm ML (defined at bregma), and -2.6 mm DV (defined at skull surface at site).

Placement of the LV cannula was confirmed by elevation of at least 100% of baseline glycemia following infusion of 210 µg (2 µL) of 5-thio-D-glucose (5TG) through the cannula using an injector extending 2 mm beyond the end of the cannula guide⁷¹. In animals that failed to present the glycemic response, the test was repeated with a 2.5 mm injector, and upon passing the 5TG test, 2.5 mm injectors were used for the remainder of the study.

For assessment in the foraging-related spatial memory task and meal pattern analysis, measures were performed 1 h following LV infusion (2 µL) of artificial cerebrospinal fluid (Veh) or clozapine-N-oxide (CNO; 18 mmol).

Single nucleus RNA sequencing

Following a 24 h fast, rats were offered a 30 min access to chow pellets (Fed) or not (Fast), 90 min prior to sacrifice. Under anesthesia via an intramuscular injection of an anesthesia cocktail (ketamine 90 mg/kg body weight [BW], xylazine, 2.8 mg/kg BW and acepromazine and 0.72 mg/kg BW), fresh brains were harvested, and flash frozen in isopentane surrounded by dry ice. Coronal sections (250 µm) were made on a cryostat and bilateral microdissections of the HPCv were obtained using a tissue puncher (2 mm diameter). Nuclei suspensions were generated from the frozen samples and data, similar to our prior descriptions⁷²⁻⁷⁴. Nuclei were processed for the 10x Genomics 3' gene expression assay (v3.1) per manufacturer protocols, and 10x Genomics Cell Ranger was used to align sequencing reads. Filtered read count matrixes were merged via Seurat, and nuclei with high UMI, low gene count and >5% mitochondrial reads were removed as doublets or low quality as we previously described⁷⁴. Counts were normalized to 10,000 reads per nucleus and scaled, and variable genes were identified mean.var.plot method in the FindVariableFeatures function in Seurat. The first 50 principal components were used to create a nearest neighbors graph and the data was then clustered at a resolution of 0.8. Subsequent quality control steps removed a cluster with abnormally low UMI, a cluster with mixed cell type markers, and three clusters with most nuclei contributed by only 1-2 samples. The remaining data was normalized and scaled again, clustered at a resolution of 0.15, resulting in identification of 17 clusters across 38,138 nuclei. Clusters were identified by expression of major cell type markers: microglia—*Cx3cr1*; macrophages—*Mrc1*; endothelial cells—*Cldn5*; astrocytes—*Gja1*; oligodendrocyte precursor cells—*Pdgfra*; oligodendrocytes—*Mag*; neurons—*Snap25*; excitatory neurons—*Slc17a6*, *Slc17a7*; granule cells—*Prox1*; inhibitory neurons—*Gad1*. Differential gene expression analysis

between the two experimental groups was performed within each cluster using a Wilcoxon rank sum test and p-values were adjusted for multiple testing using a Bonferroni correction for the total number of genes in the data set.

Pharmacological manipulations of ventral hippocampus serotonin receptor type 2a

Rats were anesthetized via an intramuscular injection of an anesthesia cocktail (ketamine 90 mg/kg body weight [BW], xylazine, 2.8 mg/kg BW and acepromazine and 0.72 mg/kg BW). Indwelling cannulae were bilaterally implanted in the CA1v, at the following stereotaxic coordinates: -4.9 mm AP (defined at bregma), ± 4.8 mm ML (defined at bregma), and -5.8 mm (defined at skull surface at site). Cannulae were fixed to the skull using jeweler's screws, instant adhesive glue and dental cement.

For assessment in the foraging-related spatial memory task and meal pattern analysis, measures were performed 5 min following CA1v infusion (200 nL/side) of 33% DMSO in artificial cerebrospinal fluid (Veh) or the serotonin type 2a receptor antagonist M100907 (1 μ g/side; M3324, Sigma-Aldrich).

Cannula placement was confirmed post-mortem via a 200 nL infusion of 2% Chicago sky blue ink through the guide cannula. Data from animals with dye confined to the CA1v were included in the analyses.

Meal pattern analysis

The Biodaq automated food intake monitoring cage system (Research Diets, New Brunswick, USA) was used to assess 24 h food intake, meal size, meal frequency and post-meal intervals. Daily average measures for the dTA-induced ablation cohort were taken over 5 consecutive days. Two 24 h measures spaced a week apart were conducted for meal pattern analysis in the CA1v-to-LHA chemogenetic silencing (VEH vs CNO) and CA1v 5HT2aR antagonism (VEH vs M100907) experiments. Meal parameters were set at a minimum meal size of 0.2 g and inter-meal interval of 900 s⁷⁵.

Immunohistochemistry

Rats received an intramuscular injection of an anesthesia cocktail (ketamine 90 mg/kg BW xylazine, 2.8 mg/kg BW and acepromazine and 0.72 mg/kg BW) prior to transcardiac perfusion with 0.9% sterile saline (pH 7.4) followed by 4% paraformaldehyde (PFA) in 0.1 M borate buffer (pH 9.5; PFA). Harvested brains were post-fixed in PFA with 12% sucrose for 24 h, then flash frozen in isopentane cooled in dry ice. Coronal sections (30 μ m) were obtained using a microtome, collected in 5-series and stored in antifreeze solution at -20 °C until further processing.

To amplify the native GFP signal in axonal projections from animals undergoing 4-OHT-induced expression of GFP under the Fed or Fasted state, the chicken anti-GFP primary antibody (1:500; Ab13970, Abcam, Boston USA) was used followed by a donkey anti-chicken secondary antibody conjugated to AF488 (1:500; AB_2340375, Jackson Immunoresearch, West Grove, USA).

To amplify the native mCherry signal from animals undergoing CA1v-to-LHA chemogenetic silencing, the rabbit anti-RFP primary antibody (1:2000; AB_2209751, Rockland, Limerick, USA) was used followed by a donkey anti-rabbit secondary antibody conjugated to Cy3 (1:500; AB_2307443, Jackson Immunoresearch).

To measure cFos protein expression in the CA1v under the Fed and Fasted state, the mouse anti-c-Fos primary antibody (1:1000; Ab208942, Abcam) was used followed by a donkey anti-mouse secondary antibody conjugated to AF647 (1:500; Jackson Immunoresearch).

Antibodies were prepared in 0.02 M potassium phosphate buffered saline (KPBS) solution containing 0.2% bovine serum albumin and 0.3% Triton X-100 at 4 °C overnight. After thorough washing with

0.02 M KPBS, sections were incubated at 4 °C overnight in secondary antibody solution. Sections were mounted and coverslipped using 50% glycerol in 0.02 M KPBS and the edges were sealed with clear nail polish. Photomicrographs were acquired using a Nikon 80i (Nikon DSQIL1280 \times 1024 resolution, 1.45 megapixel) under epifluorescence or darkfield illumination, as described previously³¹.

Fluorescent in situ hybridization

Rats received an intramuscular injection of an anesthesia cocktail (ketamine 90 mg/kg BW xylazine, 2.8 mg/kg BW and acepromazine and 0.72 mg/kg BW) prior to transcardiac perfusion with 0.9% sterile saline (pH 7.4) followed by 4% paraformaldehyde (PFA) in 0.1 M borate buffer (pH 9.5; PFA). Fluorescent in situ hybridization analyses for cFos (ACD, 403591, Newark, USA) and Htr2a (ACD, 424551) were performed in HPCv coronal sections from rats perfused under a Fed or Fasted state. Co-localization of cFos positive cells with Htr2a in the CA1v was quantitatively analyzed.

Effort-based lever pressing

Using operant conditioning boxes (Med Associates Inc, St Albans, USA), rats were trained to lever press for 45 mg sucrose pellets (Bio-Serv, F0023) over the course of 6 days with 1 session each day (2 days of fixed ratio 1 with autoshaping procedure, 2 days of fixed ratio 1 and 2 days of fixed ratio 3 reinforcement schedule). For the test session, rats were placed in the chambers to lever press for sucrose under a progressive ratio reinforcement schedule. The response requirement increased progressively using the following formula: $F(i) = 5e^{0.2i-5}$, where $F(i)$ is the number of lever presses required for the next pellet at i = pellet number and the breakpoint was defined as the final completed lever press requirement that preceded a 20-min period without earning a reinforcer, as described previously^{12,31}.

Zero-maze

Rats were placed on an elevated circular track consisting of 2 open zones (3 cm high curbs) and 2 closed zones (17.5 cm high walls) and left to explore for 5 min during the dark cycle. The total time spent in open zones (defined as body center in open sections) was measured using the AnyMaze Behavior Tracking Software (Stoelting).

Statistics and reproducibility

Data are expressed as mean \pm SEM. Differences were considered statistically significant at $p < 0.05$. All variables were analyzed, and all graphs were created using the GraphPad Prism 9 software.

Two-tailed paired t-test as used to compare changes in CA1v calcium activity dynamics during eating bouts versus interbout intervals, while two-tailed unpaired t-tests were used to compare the number of cFos+ cells, as well as number of Htr2a+ and cFos+ cells, under the Fed and Fasted states. A simple linear regression analysis was conducted to investigate the relationship between CA1v increases in calcium-dependent activity during interbout intervals and performance in the foraging-related spatial memory task. A two-way ANOVA (group \times condition) was used to analyze overlap of GFP with cFos in animals injected with 4OHT under a Fed (Fed^{GFP}) or Fasted (Fasted^{GFP}) state and perfused under a matched or mismatched condition. Repeated measures two-way ANOVAs (group \times time) were employed to assess body weight and acquisition in both the foraging-related and escape-based spatial memory tasks (errors and latencies) in the TRAP ablation (4OHT-induced dTA expression) experiments. A repeated measure two-way ANOVA (group \times time) was also used to assess acquisition in the foraging-related memory task in the chemogenetic silencing of the CA1v-to-LHA pathway and CA1v 5HT2aR antagonism experiments. A Kruskal-Wallis test with Dunn's posthoc comparison was employed to assess performance in the foraging-related spatial memory task in the TRAP ablation experiment. One-way ANOVAs were used to compare the number of GFP+ cell bodies tagged under the

Fasted, Fed or Coyote state, as well as meal pattern analysis, performance in the effort-based lever pressing task and zero-maze in the TRAP ablation cohort. Two-tailed unpaired t-test were employed to assess the number of tagged cell bodies, percentage of projection overlap and cFos overlap in the retrograde tracing experiment. Two-tailed unpaired t-test were also employed to assess performance in the escape-based spatial memory task for the TRAP ablation cohort and foraging-related spatial memory task in the TRAP Coyote, CA1v-to-LHA chemogenetic and CA1v 5HT2aR antagonism experiments. Two-tailed paired t-tests were employed to evaluate meal patterns in the CA1v-to-LHA chemogenetic and the CA1v 5HT2aR antagonism experiments.

Significant ANOVAs were analyzed with a Tukey posthoc test, where appropriate. Outliers were identified as being more extreme than the median ± 1.5 * interquartile range. For all experiments, assumptions of normality, homogeneity of variance (HOV), and independence were met where required. Behavioral and anatomical experiments were not replicated.

Reporting summary

Further information on research design is available in the Nature Portfolio Reporting Summary linked to this article.

Data availability

All data generated and analyzed for this manuscript are available from the corresponding author (SEK) upon request. The data are also available in the Open Science Framework Repository (DOI 10.17605/OSF.IO/GX3NU) and the Gene Expression Omnibus (GSE295314). Source data are provided with this paper.

References

- Higgs, S. Memory and its role in appetite regulation. *Physiol. Behav.* **85**, 67–72 (2005).
- Brunstrom, J. M. et al. Episodic memory and appetite regulation in humans. *PLoS One* **7**, e50707 (2012).
- Higgs, S. & Donohoe, J. E. Focusing on food during lunch enhances lunch memory and decreases later snack intake. *Appetite* **57**, 202–206 (2011).
- Collins, R. & Stafford, L. D. Feeling happy and thinking about food. Counteractive effects of mood and memory on food consumption. *Appetite* **84**, 107–112 (2015).
- Parent, M. B., Higgs, S., Cheke, L. G. & Kanoski, S. E. Memory and eating: a bidirectional relationship implicated in obesity. *Neurosci. Biobehav. Rev.* **132**, 110–129 (2022).
- Higgs, S. Memory for recent eating and its influence on subsequent food intake. *Appetite* **39**, 159–166 (2002).
- Kanoski, S. E. & Grill, H. J. Hippocampus contributions to food intake control: mnemonic, neuroanatomical, and endocrine mechanisms. *Biol. Psychiatry* **81**, 748–756 (2017).
- Barbosa, D. A. N. et al. An orexigenic subnetwork within the human hippocampus. *Nature* **621**, 381–388 (2023).
- Kanoski, S. E. et al. Hippocampal leptin signaling reduces food intake and modulates food-related memory processing. *Neuropsychopharmacology* **36**, 1859–1870 (2011).
- Kanoski, S. E., Fortin, S. M., Ricks, K. M. & Grill, H. J. Ghrelin signaling in the ventral hippocampus stimulates learned and motivational aspects of feeding via PI3K-Akt signaling. *Biol. Psychiatry* **73**, 915–923 (2013).
- Hsu, T. M. et al. Hippocampus ghrelin signaling mediates appetite through lateral hypothalamic orexin pathways. *Elife* **4**, e11190 (2015).
- Hsu, T. M., Hahn, J. D., Konanur, V. R., Lam, A. & Kanoski, S. E. Hippocampal GLP-1 receptors influence food intake, meal size, and effort-based responding for food through volume transmission. *Neuropsychopharmacology* **40**, 327–337 (2015).
- Noble, E. E. et al. Hypothalamus-hippocampus circuitry regulates impulsivity via melanin-concentrating hormone. *Nat. Commun.* **10**, 4923 (2019).
- Suarez, A. N., Liu, C. M., Cortella, A. M., Noble, E. E. & Kanoski, S. E. Ghrelin and orexin interact to increase meal size through a descending hippocampus to hindbrain signaling pathway. *Biol. Psychiatry* **87**, 1001–1011 (2020).
- Hannapel, R. C., Henderson, Y. H., Nalloor, R., Vazdarjanova, A. & Parent, M. B. Ventral hippocampal neurons inhibit postprandial energy intake. *Hippocampus* **27**, 274–284 (2017).
- Hannapel, R. et al. Postmeal optogenetic inhibition of dorsal or ventral hippocampal pyramidal neurons increases future intake. *eNeuro* **6**, ENEURO.0457-18.2018 (2019).
- Tonegawa, S., Pignatelli, M., Roy, D. S. & Ryan, T. J. Memory engram storage and retrieval. *Curr. Opin. Neurobiol.* **35**, 101–109 (2015).
- Josselyn, S. A. & Tonegawa, S. Memory engrams: recalling the past and imagining the future. *Science* **367**, eaaw4325 (2020).
- Nonaka, A. et al. Synaptic plasticity associated with a memory engram in the basolateral amygdala. *J. Neurosci.* **34**, 9305–9309 (2014).
- Rashid, A. J. et al. Competition between engrams influences fear memory formation and recall. *Science* **353**, 3830, 31, 3–387 (2016).
- Zhang, X., Kim, J. & Tonegawa, S. Amygdala reward neurons form and store fear extinction memory. *Neuron* **105**, 1077–1093.e7 (2020).
- Liu, X. et al. Optogenetic stimulation of a hippocampal engram activates fear memory recall. *Nature* **484**, 381–385 (2012).
- Ramirez, S. et al. Creating a false memory in the hippocampus. *Science* **341**, 387–391 (2013).
- Chen, B. K. et al. Artificially enhancing and suppressing hippocampus-mediated memories. *Curr. Biol.* **29**, 1885–1894.e4 (2019).
- Zhang, T. R. et al. Negative memory engrams in the hippocampus enhance the susceptibility to chronic social defeat stress. *J. Neurosci.* **39**, 7576–7590 (2019).
- Terranova, J. I. et al. Hippocampal-amygdala memory circuits govern experience-dependent observational fear. *Neuron* **110**, 1416–1431.e13 (2022).
- Zhou, Y. et al. A ventral CA1 to nucleus accumbens core engram circuit mediates conditioned place preference for cocaine. *Nat. Neurosci.* **22**, 1986–1999 (2019).
- Redondo, R. L. et al. Bidirectional switch of the valence associated with a hippocampal contextual memory engram. *Nature* **513**, 426–430 (2014).
- Shpokayte, M. et al. Hippocampal cells segregate positive and negative engrams. *Commun. Biol.* **5**, 1–15 (2022).
- Okuyama, T., Kitamura, T., Roy, D. S., Itohara, S. & Tonegawa, S. Ventral CA1 neurons store social memory. *Science* **353**, 1536–1541 (2016).
- Décarie-Spain, L. et al. Ventral hippocampus-lateral septum circuitry promotes foraging-related memory. *Cell Rep.* **40**, 111402 (2022).
- Jimenez, J. C. et al. Anxiety cells in a hippocampal-hypothalamic circuit. *Neuron* **97**, 670–683.e6 (2018).
- Kosugi, K. et al. Activation of ventral CA1 hippocampal neurons projecting to the lateral septum during feeding. *Hippocampus* **31**, 294–304 (2021).
- Sweeney, P. & Yang, Y. An excitatory ventral hippocampus to lateral septum circuit that suppresses feeding. *Nat. Commun.* **6**, 1–11 (2015).
- Yoshida, K., Drew, M. R., Mimura, M. & Tanaka, K. F. Serotonin-mediated inhibition of ventral hippocampus is required for sustained goal-directed behavior. *Nat. Neurosci.* **22**, 770–777 (2019).
- Henderson, Y. O., Smith, G. P. & Parent, M. B. Hippocampal neurons inhibit meal onset. *Hippocampus* **23**, 100–107 (2013).

37. Yang, A. K., Mendoza, J. A., Lafferty, C. K., Lacroix, F. & Britt, J. P. Hippocampal input to the nucleus accumbens shell enhances food palatability. *Biol. Psychiatry* **87**, 597–608 (2020).
38. Hsu, T. M. et al. A hippocampus to prefrontal cortex neural pathway inhibits food motivation through glucagon-like peptide-1 signaling. *Mol. Psychiatry* **23**, 1555–1565 (2018).
39. Rossi, M. A. & Stuber, G. D. Overlapping brain circuits for homeostatic and hedonic feeding. *Cell Metab.* **27**, 42–56 (2018).
40. Diano, S. et al. Ghrelin controls hippocampal spine synapse density and memory performance. *Nat. Neurosci.* **9**, 381–388 (2006).
41. Wee, R. W. S. et al. Internal-state-dependent control of feeding behavior via hippocampal ghrelin signaling. *Neuron* **112**, 288–305.e7 (2024).
42. Holt, M. K., Llewellyn-Smith, I. J., Reimann, F., Gribble, F. M. & Trapp, S. Serotonergic modulation of the activity of GLP-1 producing neurons in the nucleus of the solitary tract in mouse. *Mol. Metab.* **6**, 909–921 (2017).
43. D’Agostino, G. et al. Nucleus of the solitary tract serotonin 5-HT_{2C} receptors modulate food intake. *Cell Metab.* **28**, 619–630.e5 (2018).
44. Leon, R. M. et al. Hypophagia induced by hindbrain serotonin is mediated through central GLP-1 signaling and involves 5-HT_{2C} and 5-HT₃ receptor activation. *Neuropsychopharmacology* **44**, 1742–1751 (2019).
45. Herbeth, B. et al. Polymorphism of the 5-HT_{2A} receptor gene and food intakes in children and adolescents: the Stanislas Family Study. *Am. J. Clin. Nutr.* **82**, 467–470 (2005).
46. Prado-Lima, P. S., Cruz, I. B. M., Schwanke, C. H. A., Netto, C. A. & Licinio, J. Human food preferences are associated with a 5-HT_{2A} serotonergic receptor polymorphism [2]. *Mol. Psychiatry* **11**, 889–891 (2006).
47. Douglass, A. M. et al. Central amygdala circuits modulate food consumption through a positive-valence mechanism. *Nat. Neurosci.* **20**, 1384–1394 (2017).
48. Peters, C. et al. Transcriptomics reveals amygdala neuron regulation by fasting and ghrelin thereby promoting feeding. *Sci. Adv.* **9**, eadf6521 (2023).
49. Schott, B. H. et al. Genetic variation of the serotonin 2a receptor affects hippocampal novelty processing in humans. *PLoS One* **6**, 1–6 (2011).
50. Sigmund, J. C., Vogler, C., Huynh, K. D., de Quervain, D. J. F. & Papassotiropoulos, A. Fine-mapping at the HTR2A locus reveals multiple episodic memory-related variants. *Biol. Psychol.* **79**, 239–242 (2008).
51. Gong, P. et al. Variations in 5-HT_{2A} influence spatial cognitive abilities and working memory. *Can. J. Neurol. Sci.* **38**, 303–308 (2011).
52. Bekinschtein, P., Renner, M. C., Gonzalez, M. C. & Weisstaub, N. Role of medial prefrontal cortex serotonin 2A receptors in the control of retrieval of recognition memory in rats. *J. Neurosci.* **33**, 15716–15725 (2013).
53. Stackman, R. W. et al. Stimulation of serotonin 2A receptors facilitates consolidation and extinction of fear memory in C57BL/6J mice. *Neuropharmacology* **64**, 403–413 (2013).
54. Li, L. B. et al. Activation of serotonin_{2A} receptors in the medial septum-diagonal band of Broca complex enhanced working memory in the hemiparkinsonian rat. *Neuropharmacology* **91**, 23–33 (2015).
55. Zhang, G. et al. Examination of the hippocampal contribution to serotonin 5-HT_{2A} receptor-mediated facilitation of object memory in C57BL/6J mice. *Neuropharmacology* **109**, 332–340 (2016).
56. Morici, J. F. et al. 5-HT_{2a} receptor in mPFC influences context-guided reconsolidation of object memory in perirhinal cortex. *Elife* **7**, 1–23 (2018).
57. Morici, J. F. et al. Serotonin type 2a receptor in the prefrontal cortex controls perirhinal cortex excitability during object recognition memory recall. *Neuroscience* **497**, 196–205 (2022).
58. Surowka, P., Noworyta, K., Smaga, I., Filip, M. & Rygula, R. Trait sensitivity to negative feedback in rats is associated with increased expression of serotonin 5-HT_{2A} receptors in the ventral hippocampus. *Front. Mol. Neurosci.* **16**, 1092864 (2023).
59. Berumen, L. C., Rodríguez, A., Miledi, R. & García-Alcocer, G. Serotonin receptors in hippocampus. *Sci. World J.* **2012**, 823493 (2012).
60. Vertes, R. P. A PHA-L analysis of ascending projections of the dorsal raphe nucleus in the rat. *J. Comp. Neurol.* **313**, 643–668 (1991).
61. Flores, R. A. et al. Evaluation of food intake and Fos expression in serotonergic neurons of raphe nuclei after intracerebroventricular injection of adrenaline in free-feeding rats. *Brain Res.* **1678**, 153–163 (2018).
62. Li, Y. et al. Serotonin neurons in the dorsal raphe nucleus encode reward signals. *Nat. Commun.* **7**, 1–15 (2016).
63. Thanarajah, S. E. et al. Food intake recruits orosensory and post-ingestive dopaminergic circuits to affect eating desire in humans. *Cell Metab.* **29**, 695–706.e4 (2019).
64. Azevedo, E. P. et al. A role of Drd2 hippocampal neurons in context-dependent food intake. *Neuron* **102**, 873–886.e5 (2019).
65. Rozin, P., Dow, S., Moscovitch, M. & Rajaram, S. What causes humans to begin and end a meal? A role for memory for what has been eaten, as evidenced by a study of multiple meal eating in amnesic patients. *Psychol. Sci.* **9**, 392–396 (1998).
66. McDougale, M. et al. Separate gut-brain circuits for fat and sugar reinforcement combine to promote overeating. *Cell Metab.* **36**, 393–407.e7 (2024).
67. Goldstein, N. et al. Hypothalamic detection of macronutrients via multiple gut-brain pathways. *Cell Metab.* **33**, 676–687.e5 (2021).
68. Subramanian, K. S. et al. Hypothalamic melanin-concentrating hormone neurons integrate food-motivated appetitive and consummatory processes in rats. *Nat. Commun.* **14**, 1–14 (2023).
69. Oh, S. W. et al. A mesoscale connectome of the mouse brain. *Nature* **508**, 207 (2014).
70. Giannotti, G., Heinsbroek, J. A., Yue, A. J., Deisseroth, K. & Peters, J. Prefrontal cortex neuronal ensembles encoding fear drive fear expression during long-term memory retrieval. *Sci. Rep.* **9**, 10709 (2019).
71. Ritter, R. C., Slusser, P. G. & Stone, S. Glucoreceptors controlling feeding and blood glucose: location in the hindbrain. *Science* **213**, 451–452 (1981).
72. Reiner, B. C. et al. Single nuclei RNA sequencing of the rat AP and NTS following GDF15 treatment. *Mol. Metab.* **56**, 101422 (2022).
73. Reiner, B. C. et al. Single nucleus transcriptomic analysis of rat nucleus accumbens reveals cell type-specific patterns of gene expression associated with volitional morphine intake. *Transl. Psychiatry* **12**, 374 (2022).
74. Borner, T. et al. GIP receptor agonism blocks chemotherapy-induced nausea and vomiting. *Mol. Metab.* **73**, 101743 (2023).
75. Farley, C., Cook, J. A., Spar, B. D., Austin, T. M. & Kowalski, T. J. Meal pattern analysis of diet-induced obesity in susceptible and resistant rats. *Obes. Res.* **11**, 845–851 (2003).
76. Swanson, L. W. Brain maps 4.0—structure of the rat brain: an open access atlas with global nervous system nomenclature ontology and flatmaps. *J. Comp. Neurol.* **526**, 935–943 (2018).

Acknowledgements

This work was supported by a Quebec Research Funds Postdoctoral Fellowship (315201) and an Alzheimer’s Association Research Fellowship to promote diversity (AARFD-22-972811) to L.D.S., a National Science Foundation Graduate Research Fellowship to K.S.S. and National Institute of Diabetes and Digestive and Kidney Diseases grants: DK105155 to M.R.H. and DK104897 to S.E.K. Clozapine-N-Oxide was kindly provided by the National Institute of Mental Health.

Author contributions

L.D.S. and S.E.K. conceived and performed the experiments and wrote the manuscript. C.G., L.T.L., K.S.S., A.E.K., S.X.G., I.D., A.G.B., M.E.K., J.J.R., A.I.W., A.H.G., O.M., and K.N.D. performed experiments. S.N.C., R.C.C., B.C.R., and M.R.H. performed experiments and provided expertise on experimental design. M.Y., G.d.L. and K.P.M. provided expertise on experimental design.

Competing interests

B.C.R. and M.R.H. both receive research funding from Novo Nordisk and Boehringer Ingelheim that was not used in support of these studies. M.R.H. receives research funding from Eli Lilly & Co., Gila Therapeutics, and Pfizer that was not used in support of these studies. All other authors declare no competing interests.

Additional information

Supplementary information The online version contains supplementary material available at <https://doi.org/10.1038/s41467-025-59687-1>.

Correspondence and requests for materials should be addressed to Scott E. Kanoski.

Peer review information *Nature Communications* thanks the anonymous reviewer(s) for their contribution to the peer review of this work. A peer review file is available.

Reprints and permissions information is available at <http://www.nature.com/reprints>

Publisher's note Springer Nature remains neutral with regard to jurisdictional claims in published maps and institutional affiliations.

Open Access This article is licensed under a Creative Commons Attribution-NonCommercial-NoDerivatives 4.0 International License, which permits any non-commercial use, sharing, distribution and reproduction in any medium or format, as long as you give appropriate credit to the original author(s) and the source, provide a link to the Creative Commons licence, and indicate if you modified the licensed material. You do not have permission under this licence to share adapted material derived from this article or parts of it. The images or other third party material in this article are included in the article's Creative Commons licence, unless indicated otherwise in a credit line to the material. If material is not included in the article's Creative Commons licence and your intended use is not permitted by statutory regulation or exceeds the permitted use, you will need to obtain permission directly from the copyright holder. To view a copy of this licence, visit <http://creativecommons.org/licenses/by-nc-nd/4.0/>.

© The Author(s) 2025